Sterol carrier protein-2 deficiency attenuates diet-induced dyslipidemia and atherosclerosis in mice

Received for publication, February 5, 2018, and in revised form, April 25, 2018 Published, Papers in Press, April 26, 2018, DOI 10.1074/jbc.RA118.002290

Hongliang He[‡], Jing Wang[‡], Paul J. Yannie[§], Genta Kakiyama[§], William J. Korzun[¶], and Shobha Ghosh[‡§1]

From the Departments of [‡]Internal Medicine and [¶]Clinical and Laboratory Sciences, Virginia Commonwealth University (VCU) Medical Center, Richmond, Virginia 23298 and the [§]Hunter Homes McGuire Veterans Affairs Medical Center, Richmond, Virginia 23249

Edited by George M. Carman

Intracellular cholesterol transport proteins move cholesterol to different subcellular compartments and thereby regulate its final metabolic fate. In hepatocytes, for example, delivery of high-density lipoprotein (HDL)–associated cholesterol for bile acid synthesis or secretion into bile facilitates cholesterol elimination from the body (anti-atherogenic effect), whereas delivery for esterification and subsequent incorporation into apolipoprotein B–containing atherogenic lipoproteins (*e.g.* very-low-density lipoprotein (VLDL)) enhances cholesterol secretion into the systemic circulation (pro-atherogenic effect). Intracellular cholesterol transport proteins such as sterol carrier protein-2 (SCP2) should, therefore, play a role in regulating these pro- or anti-atherosclerotic processes. Here, we sought to evaluate the effects of SCP2 deficiency on the development of diet-induced atherosclerosis. We generated LDLR$^{-/-}$ mice deficient in SCP2/SCPx (LS) and examined the effects of this deficiency on Western diet–induced atherosclerosis. SCP2/SCPx deficiency attenuated atherosclerosis in LS mice by >80% and significantly reduced plasma cholesterol and triglyceride levels. Investigation of the likely underlying mechanisms revealed a significant reduction in intestinal cholesterol absorption (given as an oral gavage) in SCP2/SCPx-deficient mice. Consistently, siRNA-mediated knockdown of SCP2 in intestinal cells significantly reduced cholesterol uptake. Furthermore, hepatic triglyceride/VLDL secretion from the liver or hepatocytes isolated from SCP2/SCPx-deficient mice was significantly reduced. These results indicate an important regulatory role for SCP2 deficiency in attenuating diet-induced atherosclerosis by limiting intestinal cholesterol absorption and decreasing hepatic triglyceride/VLDL secretion. These findings suggest targeted inhibition of SCP2 as a potential therapeutic strategy to reduce Western diet–induced dyslipidemia and atherosclerosis.

Hydrophobicity of nonesterified or free cholesterol (FC)[2] precludes its free movement within the cell and between different cellular membranes, a process that is essential to multiple cellular functions, including FC esterification, conversion to bile acids in hepatocytes, or synthesis of steroid hormones in steroidogenic tissues. Although release of FC from the donor membrane is typically rate-limiting, and physical proximity with the acceptor membrane is not required (1, 2), transfer of FC between membranes is enhanced by intracellular transfer/carrier proteins, such as members of the steroidogenic acute regulatory (StAR) family (3), which are highly specific for sterols, or nonspecific transporters including sterol carrier protein 2 (SCP2) and fatty acid binding protein 1 (FABP1) (4, 5). Consequently, these transfer proteins not only regulate the distribution of cholesterol in cell organelles but also play an important role in intracellular cholesterol metabolism and tissue-specific distribution. Furthermore, expression of these proteins is closely related to the rate of cholesterol metabolism in each tissue (6). Therefore, the role of these proteins is extensively studied in steroidogenic tissues such as adrenals (where these proteins regulate steroid hormone synthesis by modulating the delivery of FC to appropriate subcellular organelles) and the liver (the principal organ responsible for maintaining whole-body cholesterol homeostasis).

The Scp2 gene encodes the 58-kDa sterol carrier protein-x (SCPx) and 15-kDa pro-SCP2 proteins, both of which contain a 13-kDa SCP2 domain in their C termini. SCPx is localized primarily to peroxisomes and functions as a thiolase. Pro-SCP2 can either be obtained by proteolytic cleavage of SCPx, or it is independently transcribed using an internal/alternate transcription start site (7). Mature SCP2 (13 kDa), representing the C-terminal end of SCPx, as well as pro-SCP2 is, however, obtained by proteolytic cleavage. Mechanisms that regulate transcription initiation from the internal start site to directly generate pro-SCP2 or proteolytic cleavage of SCPx or pro-SCP2 to generate mature SCP2 are not completely defined.

In addition to being involved in maintaining differential cholesterol content of the plasma membrane leaflets (8), replenishing mitochondrial membrane cholesterol (9), and regulating lipid rafts and signaling (10), SCP-2 is also involved in regulating hepatic cholesterol homeostasis. Niemann–Pick C disease, characterized by hepatic cholesterol accumulation in lyso-

This work was supported in part by National Institutes of Health Grant HL097346 and a VCU School of Medicine bridge grant award (to S. G.). The authors declare that they have no conflicts of interest with the contents of this article. The content is solely the responsibility of the authors and does not necessarily represent the official views of the National Institutes of Health.

[1] To whom correspondence should be addressed: Dept. of Internal Medicine, Division of Pulmonary and Critical Care, MMRB 6050, 1220 E. Broad St., VCU Medical Center, Richmond, VA 23298-0050. Tel.: 804-827-1012; Fax: 804-628-0325; E-mail: shobha@vcu.edu.

[2] The abbreviations used are: FC, free or unesterified cholesterol; HDL, high-density lipoprotein; CE, cholesteryl ester; DPM, disintegrations per minute; H&E, hematoxylin and eosin; VLDL, very-low-density lipoprotein; WD, Western diet; AcLDL, acetylated low-density lipoprotein; LDLR, low density lipoprotein receptor; FBS, fetal bovine serum; 7α-OOH, 7α-hydroperoxycholesterol.

somes and the Golgi, is associated with reduced levels of hepatic 13-kDa SCP2 (11). SCP2 affects hepatic cholesterol accumulation (12) and enhances HDL-mediated cholesterol uptake in primary hepatocytes (13). Earlier studies from our laboratory have demonstrated an increase in flux of cholesterol from HDL-associated cholesteryl esters (HDL-CE) to bile acids by adenovirus-mediated transient overexpression of SCP2 as well as FABP1 (14). Studies with mice lacking SCP-2/SCPx or FABP1 or both have provided evidence for the role of these two proteins in modulating biliary lipid levels (15, 16).

Given the inability of mammalian systems to metabolize the steroid nucleus, conversion of hydrophobic cholesterol to more water-soluble bile acids and solubilization of cholesterol by these detergents, followed by excretion into bile, represents a major mechanism for cholesterol elimination from the body. A homeostatic balance between cholesterol intake/*de novo* synthesis and cholesterol elimination is central to the development of atherosclerosis. Despite the significant role of intracellular cholesterol transfer proteins such as SCP-2 in regulating the expression of genes involved in hepatic cholesterol homeostasis (17), the direct role of these proteins in modulating atherogenesis has not been examined to date. Based on our earlier studies, where transient overexpression of SCP2 led to increased flux of cholesterol from HDL to bile, we speculated an anti-atherogenic role for SCP2 (14). To directly address this hypothesis, in this study we examined the effects of SCP2/SCPx deficiency on the development of Western diet–induced atherosclerosis in the LDLR$^{-/-}$ background. Contrary to the expected increase in diet-induced atherosclerosis, a dramatic attenuation of lesion development was noted in mice lacking SCP2/SCPx. Data are presented to indicate that a significant decrease in dietary cholesterol absorption in the intestine as well as in hepatic VLDL secretion by SCP2/SCPx deficiency collectively represent the mechanism underlying the observed attenuation of plasma lipid levels and, consequently, the reduction in Western diet–induced atherosclerosis in LDLR$^{-/-}$ mice.

Results

SCP2 deficiency significantly attenuates Western diet–induced atherosclerosis in LDLR$^{-/-}$ mice

Intracellular cholesterol-binding proteins facilitate delivery of cholesterol to appropriate organelles for subsequent metabolism, and we have demonstrated earlier that adenovirus-mediated overexpression of SCP2 increases the flux of cholesterol from HDL to bile and feces, indicative of a potential anti-atherogenic role of this protein (14). However, as shown in Fig. 1*A*, deficiency of SCP2/SCPx (LS) dramatically reduced diet-induced atherosclerotic lesions in LDLR$^{-/-}$ mice. Compared with LDLR$^{-/-}$ mice, the lesion area in the aortic arch in LS mice was significantly reduced in both males (37.31 ± 7.79 *versus* 6.85 ± 5.47, $p < 0.0001$) and females (29.77 ± 4.43 *versus* 14.09 ± 6.62, $p < 0.011$). Similar trends were seen when total aortic lesion areas in LS mice were compared (Fig. 1*C*) (males 19.15 ± 2.87 *versus* 3.31 ± 2.16, $p < 0.0001$; females 13.35 ± 2.68 *versus* 6.41 ± 2.36, $p < 0.0001$).

The aortic root represents another anatomical site of plaque development, and changes in plaque area at this site were also

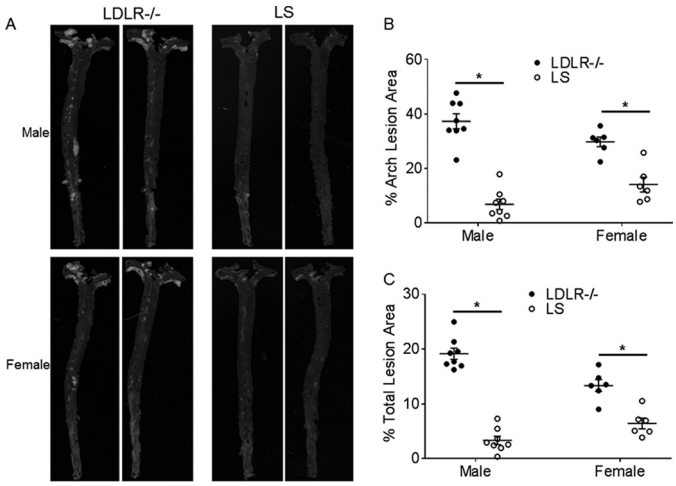

Figure 1. SCP2 deficiency significantly attenuates diet-induced atherosclerosis. At 10 weeks of age, LDLR$^{-/-}$ and LS mice were fed a high-fat, high-cholesterol–containing Western-type diet (TD88137) for 16 weeks. Aortae were dissected and prepared for *en face* analyses. The total area as well as the area occupied by the lesions was quantified using Axiovision software and expressed as percent lesion area. *A*, representative images. *B*, percent area occupied by the lesions in the aortic arch. *C*, percent area occupied by the lesions in the entire aorta. *, $p < 0.05$; individual *p* values are included in the text.

examined using H&E-stained aortic root sections. Consistent with the *en face* analyses shown in Fig. 1, a significant reduction in the area occupied by the plaque in the aortic root was noted in LS mice (Fig. 2, *A* and *B*). To evaluate changes in plaque characteristics, if any, Masson's trichrome–stained aortic root sections were analyzed to determine the percentage of necrotic area. A significant reduction in plaque necrosis was seen in LS mice (Fig. 2, *C* and *D*).

SCP2 deficiency significantly reduces total plasma cholesterol and triglyceride

Plasma cholesterol and triglyceride levels are considered a reliable marker of whole-body lipid homeostasis, and elevated levels associated with development of atherosclerosis are either the result of increased uptake of dietary lipids or enhanced hepatic secretion of pro-atherogenic ApoB–containing VLDL. SCP2 deficiency significantly reduced plasma cholesterol levels in LS mice (1747.38 ± 670.62 *versus* 543.00 ± 144.57, $p < 0.0001$ in males and 1424.33 ± 205.1 *versus* 966.83 ± 214.97, $p = 0.0118$ in females; Fig. 3*A*). Furthermore, comparison of changes in percent total cholesterol associated with non-HDL or HDL fractions showed that the observed reduction in plasma cholesterol was primarily determined by reduction in non-HDL cholesterol or cholesterol associated with LDL and VLDL fractions (86.15 ± 11.93 *versus* 71.55 ± 5.85, $p = 0.0077$ in males and 91.42 ± 1.44 *versus* 85.95 ± 2.04, $p = 0.0003$ in females, Fig. 3*B*). In contrast, there was a small but statistically significant increase in the percentage of cholesterol associated with the HDL fraction (13.85 ± 11.93 *versus* 28.45 ± 5.85, $p = 0.0077$ in males and 8.58 ± 1.44 *versus* 14.05 ± 2.04, $p = 0.0003$ in females; Fig. 3*B*). To facilitate a direct demonstration of the effects of SCP2 deficiency on cholesterol distribution between plasma lipoprotein fractions, the data are also represented after normalization to total cholesterol levels observed in LDLR$^{-/-}$ mice of the same sex. Significant reduction in non-HDL choles-

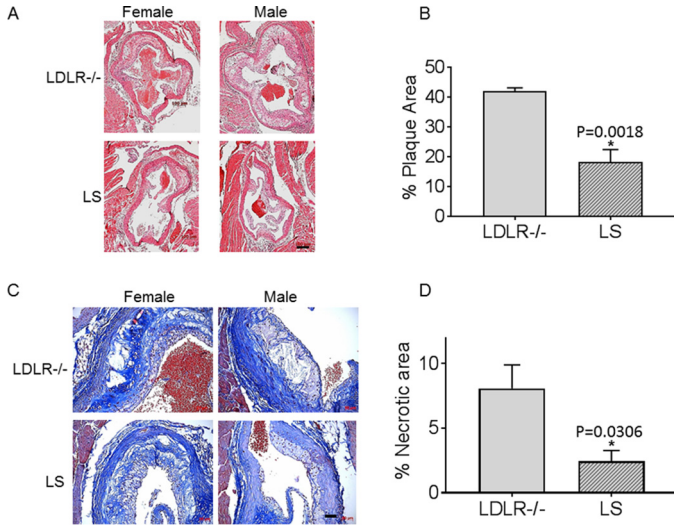

Figure 2. SCP2 deficiency reduces plaque size as well as plaque necrosis in the aortic root. Paraffin-embedded aortic root sections (5 μm) were stained with H&E or Masson's trichrome, imaged, and analyzed by Axiovision software. *A*, representative H&E stained images of the aortic root of the indicated genotypes/sex. *Scale bar* = 100 μm. *B*, the total aortic root and area occupied by the lesions was quantified, and data (mean ± S.D., $n = 6$) are presented as percent lesion area. *C*, representative trichrome-stained images of the indicated genotypes/sex. *Scale bar* = 50 μm. *D*, the total and necrotic areas were quantified for all three aortic valve leaflets, and data (mean ± S.D., $n = 12$ leaflets) are presented as percent necrotic area. *, $p < 0.05$.

terol is apparent in LS mice of both sexes (87.31 ± 32.41 *versus* 39.27 ± 11.04, $p = 0.0014$ in males and 91.39 ± 11.45 *versus* 60.78 ± 6.31, $p = 0.0002$ in females; Fig. 3*C*). It is noteworthy that, in WD-fed LDLR$^{-/-}$ mice, >90% plasma cholesterol is associated with the non-HDL fraction (18). A strong positive correlation was obtained between the total lesion area and plasma cholesterol levels (Fig. 3*D*). Plasma triglyceride levels were also significantly reduced in male LS mice (471.88 ± 292.22 *versus* 121.75 ± 48.20, $p = 0.0016$; Fig. 3*E*), but this decrease did not reach statistical significance in female mice (411.33 ± 268.1 *versus* 225.67 ± 139.25, $p = 0.1631$). Although total lesions increased with increasing plasma triglyceride levels, this correlation did not reach statistical significance (Fig. 3*F*). These data suggest that global SCP2 deficiency–mediated attenuation of plasma lipids likely underlies the observed decrease in atherosclerotic lesions in LS mice.

SCP2 deficiency significantly reduces intestinal cholesterol absorption

Diet-induced hypercholesterolemia underlies the development of atherosclerosis in this model of Western diet–induced atherosclerosis in LDLR$^{-/-}$ mice. Therefore, any reduction in absorption of dietary cholesterol is likely to affect the development of atherosclerosis. To examine whether SCP2 deficiency–mediated changes in intestinal cholesterol absorption represent the mechanism underlying the observed reduction in plasma lipids as well as atherosclerosis, the appearance of orally administered [^{3}H]cholesterol in plasma was monitored under conditions where tissue uptake of absorbed cholesterol is prevented by tyloxapol-mediated inhibition of lipoprotein lipase. A significant reduction in plasma DPM was seen in SCP2$^{-/-}$ mice (286.23 ± 60.58 *versus* 180.81 ± 11.43, $p = 0.007$ in males and 236.11 ± 71.06 *versus* 169.68 ± 35.09, $p = 0.036$ in females; Fig. 4*A*). These data suggest that SCP2/SCPx deficiency leads to reduced intestinal absorption of dietary cholesterol, resulting in attenuation of diet-induced hypercholesterolemia.

Although absorption of cholesterol occurs via NPC1L1, intestinal cells secrete cholesterol along with phytosterols back into the lumen via ABCG5/G8. Furthermore, cholesterol absorption is not uniform along the length of the intestine. Expression of NPC1L1 or ABCG5 and ABCG8 along the intestine was evaluated in WT and SCP2$^{-/-}$ mice to determine the effects SCP2 deficiency. Although no significant difference was noted in the expression of NPC1L1, there was a significant reduction in the expression of ABCG5 and ABCG8 in the distal P4 segment of the intestine of SCP2$^{-/-}$ mice (Fig. 4*B*). Consistent with global deficiency of SCP2 in these mice, no expression of SCP2 protein was noted along the length of the intestine, *i.e.* segments P1 through P4 (Fig. 4*C*).

Because the mice used in this study have a global deficiency of SCP2/SCPx, to directly assess the effects of SCP2 deficiency in intestinal cells on cholesterol absorption/uptake, SCP2 was knocked down in the human intestinal epithelial cell line HT-29 using SCP2-specific siRNA. A concentration-dependent decrease in SCP2 mRNA was noted, along with maximum reduction in SCP2 protein seen at the highest siRNA concentration tested (Fig. 4*D*). Cholesterol uptake was monitored in HT-29 cells transfected with either scrambled or SCP2 siRNA. A time-dependent increase in cholesterol uptake was seen, and this increase was significantly attenuated when SCP2 was knocked down with siRNA (Fig. 4*E*). These data indicate that deficiency of SCP2 in intestinal epithelial cells limits cholesterol absorption and likely represents the mechanism underlying the observed reduction in plasma lipids and attenuated atherosclerosis in LS mice.

SCP2 deficiency significantly reduced hepatic VLDL secretion

Upon WD feeding, increased absorbed lipids are repackaged in the liver and secreted as pro-atherogenic lipoprotein VLDL. Therefore, in addition to the effects of altered lipid absorption, changes in secretion of pro-atherogenic lipoproteins from the liver are also likely to modify plasma lipids and the downstream development of atherosclerosis. Time-dependent accumulation of VLDL-associated triglycerides in the plasma compartment following inhibition of lipoprotein lipase is routinely used to evaluate hepatic VLDL secretion. To examine whether SCP2 deficiency affects hepatic VLDL secretion, we monitored plasma triglyceride levels in WT and SCP2$^{-/-}$ mice following tyloxapol-mediated inhibition of lipoprotein lipase. As shown in Fig. 5*A*, triglyceride secretion rates calculated from the plasma triglyceride levels were significantly reduced in SCP2$^{-/-}$ mice (12.05 ± 0.73 *versus* 7.46 ± 1.03, $p = 0.0021$). These data suggest that SCP2 deficiency attenuates pro-atherogenic VLDL secretion from the liver.

Because the mice used in these studies lack SCP2 in all tissues, to confirm the effects of SCP2 deficiency on VLDL/triglyceride secretion from hepatocytes, direct secretion of triglycerides as well as cholesteryl ester into the incubation medium from primary hepatocytes isolated from WT or SCP2$^{-/-}$ mice was assessed. Secretion of [^{3}H]oleic acid–labeled triglycerides (Fig. 5*B*) as well as cholesteryl esters (Fig. 5*C*) by SCP2/SCPx-

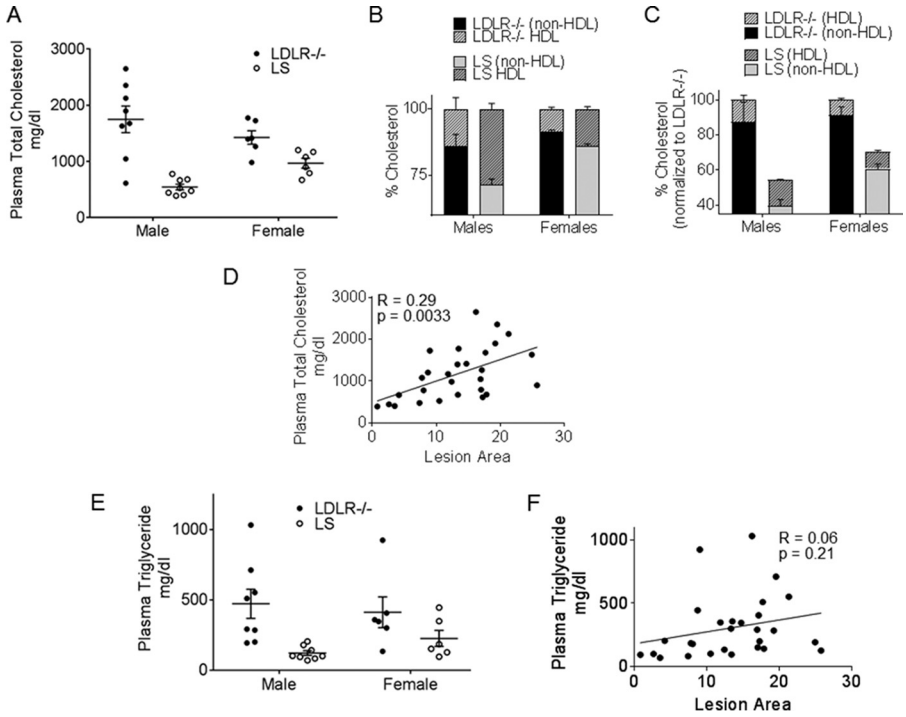

Figure 3. SCP2 deficiency significantly reduces plasma cholesterol and triglyceride levels. At 10 weeks of age, LDLR$^{-/-}$ and LS mice were fed a high-fat, high-cholesterol–containing Western-type diet (TD88137) for 16 weeks. After an overnight fast, mice were euthanized, and fasting plasma was collected. *A*, levels of total plasma cholesterol for indicated genotype and sexes. *B*, percent of total plasma cholesterol associated with the non-HDL or HDL fraction. *C*, percent of total plasma cholesterol associated with the non-HDL or HDL fraction in both genotypes normalized to total plasma cholesterol in LDLR$^{-/-}$ mice of the respective sex. *D*, linear regression analyses of total lesion area and plasma cholesterol; the observed coefficient of correlation (R) as significance of correlation (*p* value) is indicated. *E*, total plasma triglyceride for the indicated genotype and sexes. *F*, linear regression analyses of total lesion area and plasma triglyceride levels; the observed coefficients of correlation (R) as significance of correlation (*p* value) is indicated.

deficient hepatocytes was significantly reduced, confirming the reduction in hepatic secretion rates observed *in vivo*.

Reduced secretion of VLDL could potentially lead to hepatic accumulation of lipids, and therefore morphological changes in the livers of WD-fed LDLR$^{-/-}$ and LS mice were compared. Significant lipid accumulation was noted in livers from WD-fed LDLR$^{-/-}$ mice compared with LS mice, indicating that SCP2 deficiency does not lead to increased accumulation of lipids in the liver (Fig. 6*A*). Lack of SCP2 expression in livers form LS mice was confirmed by almost undetectable levels of Scp2 mRNA in LS mice (Fig. 6*B*). Consistent with lack of lipid accumulation in the liver, no significant difference in the expression of lipogenic genes (namely, ApoB, Fas, Srebp-1c, and Srebp-2) was noted between livers from WT and SCP2$^{-/-}$ mice (Fig. 6*C*).

These data indicate that SCP2/SCPx deficiency leads to reduced VLDL secretion from liver/hepatocytes and that SCP2 deficiency likely leads to reduced plasma lipids by not only limiting intestinal absorption but also by decreasing hepatic VLDL secretion. Furthermore, SCP2 deficiency also reduces WD-induced lipid accumulation in the liver without any significant change in expression of genes involved in lipogenesis.

SCP2 deficiency has limited effects on pathways involved in cholesterol elimination

An imbalance between forward transport of cholesterol to peripheral tissues and its return to the liver for final elimination underlies accumulation of lipid-laden macrophage foam cells within the artery wall. Although the data presented above provide strong evidence for SCP2 deficiency–mediated reduction in plasma lipids because of intestinal lipid absorption as well as hepatic lipid secretion, the effects of SCP2 deficiency on reverse flux of cholesterol from macrophages to the liver and final elimination in bile were also monitored to examine any direct effects of SCP2 deficiency on these processes.

Changes, if any, in the uptake of modified LDL by macrophages from WT or SCP2$^{-/-}$ were examined, and, as shown in Fig. 7*A*, no apparent difference in Oil Red O–stained neutral lipid was seen in WT control and SCP2$^{-/-}$ macrophages before or after incubation with acetylated LDL (AcLDL). Consistently, although there was an increase in total cellular cholesterol upon loading with AcLDL in both genotypes, there was no significant difference in total cellular cholesterol mass between WT and SCP2$^{-/-}$ macrophages before or after loading (Fig. 7*B*). The observed lack of difference in the expression of SR-A (Fig. 7*C*) further suggests that SCP2 deficiency does not affect the uptake of modified LDL. When efflux of cholesterol from AcLDL-loaded macrophages was measured, a small but significant reduction in cholesterol efflux was observed in LS macrophages. An increase in cholesterol efflux capacity is associated with reduction in the development of atherosclerosis, and this observed reduction in cholesterol efflux from SCP2$^{-/-}$ macrophages suggests that SCP2 deficiency in macrophages may not be the major underlying mechanism for the observed decrease in atherosclerosis in LS mice.

Final elimination of cholesterol from the body, required to maintain whole-body cholesterol homeostasis and limit devel-

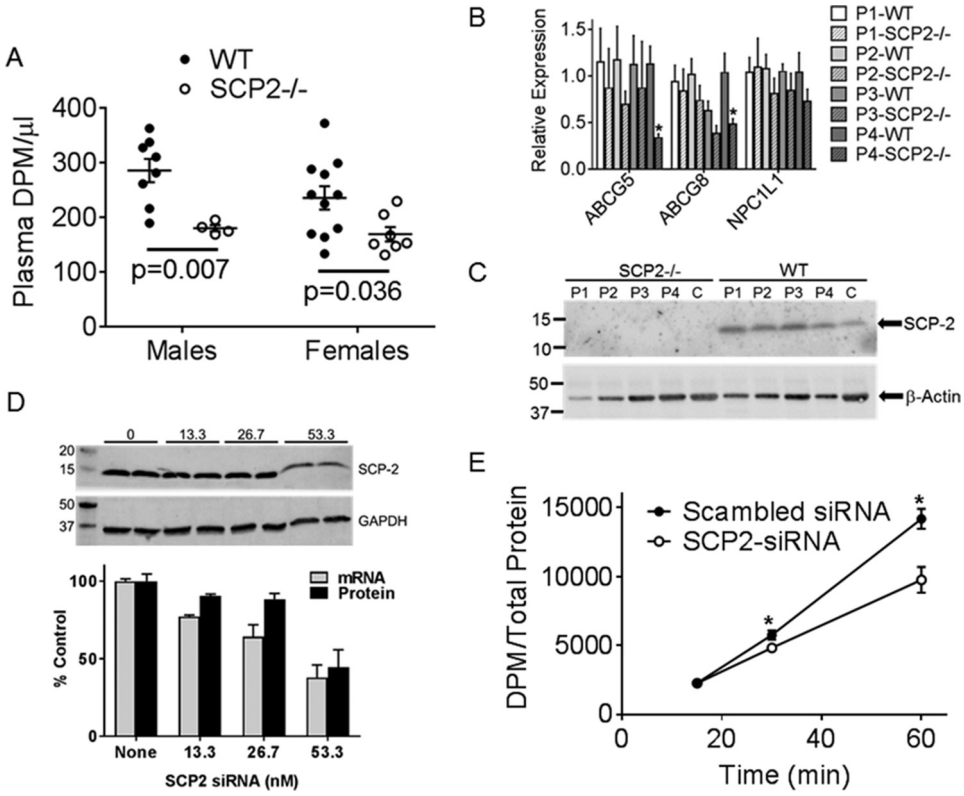

Figure 4. SCP2 deficiency significantly reduces intestinal cholesterol absorption, and SCP2 knockdown in intestinal epithelial cells reduces cholesterol uptake. *A*, C57BL/6 (WT) or SCP2$^{-/-}$ mice were injected intravenously with the lipoprotein lipase inhibitor tyloxapol (500 mg/kg body weight) and gavaged with [^{3}H]cholesterol in olive oil (2 μCi in 200 μl) after 5 min. Intestinal cholesterol absorption was assessed by monitoring the radiolabel associated with plasma collected at the time of euthanasia. Data are presented as plasma DPM per microliter of plasma for the indicated genotype and sex. *B*, the entire length of the intestine, from the base of the stomach to the tip of the cecum, was divided into four equal parts (P1 to P4), and total RNA was isolated. The mRNA levels of indicated genes were determined by real-time PCR as described under "Experimental procedures" and normalized to the housekeeping gene β-actin. *C*, total protein extracts from ileum segments P1 to P4 of WT and SCP2$^{-/-}$ mice as well as the colon (*C*) were analyzed by Western blotting for expression of SCP2; β-actin was used as the loading control. Human intestinal epithelial cells (HT-29) were transfected with scrambled or SCP2-specific siRNA as described under "Experimental procedures." Total protein or RNA was extracted and used to determine the levels of SCP2. *D*, *top*, a representative Western blot. *Bottom*, levels of SCP2 mRNA quantified by quantitative PCR and SCP2 protein by densitometric analyses of Western blots. Data are presented as percent scrambled siRNA-transfected controls for the indicated SCP2 siRNA concentrations used. *E*, HT-29 cells transfected with scrambled siRNA or 53.3 nM SCP2-specific siRNA were incubated with [^{3}H]-cholesterol, and total cellular uptake was monitored as described under "Experimental procedures." Data (mean $\pm$ S.D., $n = 6$) are presented as DPM normalized to total cellular protein. *, $p < 0.05$.

opment of atherosclerosis, occurs via biliary or nonbiliary routes. To evaluate the effects of SCP2 deficiency on modulating cholesterol elimination from the body, secreted bile acids and cholesterol were monitored in gall bladder bile and normalized to total biliary phospholipid content. Deficiency of SCP2/SCPx did not affect biliary bile acid (Fig. 8*A*) or free cholesterol (Fig. 8*B*) secretion. Although increased biliary elimination of cholesterol from the body as bile acids or free cholesterol is generally viewed as anti-atherogenic, a dramatic reduction in atherosclerosis with no change in biliary bile acids or cholesterol in LS mice points to a possible limited contribution of the cholesterol elimination pathway to the observed attenuation of atherosclerosis by deficiency of SCP2/SCPx in these global knockout mice.

Discussion

While recognizing the role of extracellular trafficking of cholesterol in the progression of atherosclerosis, Billheimer and Reinhart (19) argued more than 3 decades ago for a major role of intracellular cholesterol trafficking, possibly by regulating transport of cholesterol back to the liver from the peripheral tissues and secretion into the bile. Although ample evidence exists for defining the role of SCP2/SCPx in modulating hepatic cholesterol/bile acid metabolism, the data presented here describe, for the first time, the dramatic anti-atherogenic (>80% decrease) effects of SCP2/SCPx deficiency in atherosusceptible LDLR$^{-/-}$ mice. Furthermore, SCP2/SCPx deficiency led to a significant reduction in plasma cholesterol and triglyceride levels despite consumption of a high-fat, high-cholesterol– containing Western diet. Consistently, we demonstrate that SCP2/SCPx deficiency reduces absorption of cholesterol in the intestine and attenuates VLDL secretion from the liver, identifying SCP2 as a potential therapeutic target to modulate dyslipidemia and its downstream adverse effects.

Dyslipidemia is central to the development of atherosclerotic plaques, and LDLR$^{-/-}$ mice develop atherosclerosis only after a dietary challenge with a high-fat, high-cholesterol–containing Western diet. Therefore, the contribution of dietary lipids to overall dyslipidemia is paramount in this model of atherogenesis. Sterol carrier protein–like activity was described in the rat intestine by Kharroubi *et al.* (20), and the widespread distribution of SCP2-like protein in the intestine was thought to be related to the potential transfer functions in all phases of cholesterol processing. Wouters *et al.* (21) confirmed the

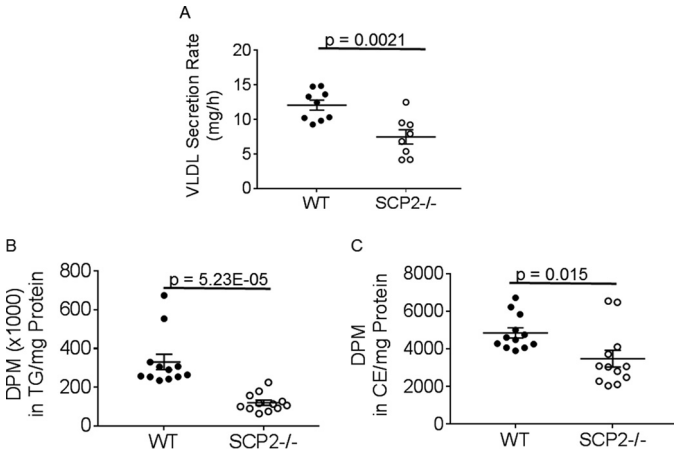

Figure 5. SCP2 deficiency significantly reduces lipid secretion from liver and isolated hepatocytes. *A*, C57BL/6 (WT) or SCP2$^{-/-}$ mice were injected with the lipoprotein lipase inhibitor tyloxapol (500 mg/kg of body weight), and blood samples were drawn at 0 and 3 h. Triglyceride secretion rates for indicated genotypes and sexes are presented. *B* and *C*, primary hepatocytes were prepared from C57BL/6 (WT) or SCP2$^{-/-}$ mice. Following incubation with [^{3}H]oleic acid, radiolabel associated with secreted triglycerides (*TG*, *B*) or cholesteryl esters (*C*) was determined as described under "Experimental procedures" and normalized to cellular protein. Data are presented as DPM associated with the triglyceride or cholesteryl ester fraction in the total lipids extracted from the medium per milligram of total protein.

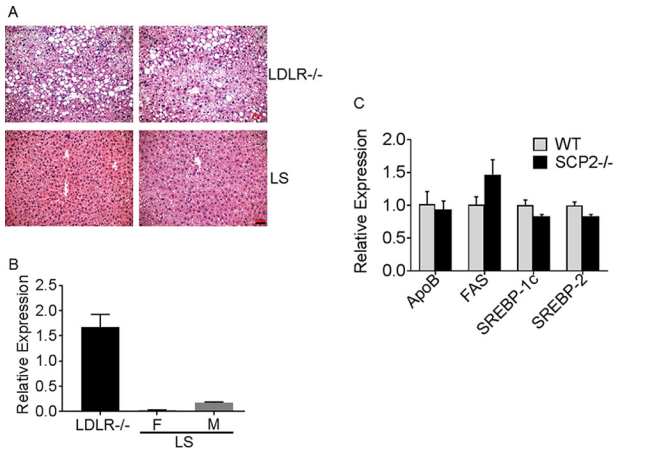

Figure 6. SCP2 deficiency leads to reduced lipid accumulation in the liver without a change in the expression of lipogenic genes. *A*, liver tissue harvested from WD-fed LDLR$^{-/-}$ or LS mice were paraffin-embedded, and 5-μm sections were stained with H&E. Images were acquired using a Zeiss inverted microscope fitted with a digital camera. *Scale bar* = 50 μm. B, SCP2 mRNA levels in total liver RNA were determined by real-time PCR as described under "Experimental procedures" and normalized to the housekeeping gene β-actin. Relative expression (mean ± S.D., $n = 6$) is shown. *C*, hepatic mRNA levels of the indicated genes were determined by real-time PCR as described under "Experimental procedures" and normalized to the housekeeping gene β-actin. Relative expression (mean ± S.D., $n = 6$) is shown.

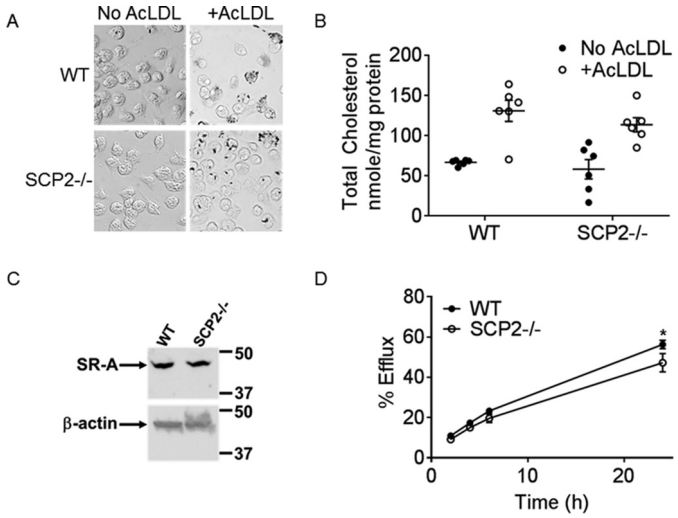

Figure 7. Effects of SCP2 deficiency on cholesterol accumulation in and cholesterol efflux from macrophages. Thioglycolate-elicited macrophages were isolated from C57BL/6 (WT) and SCP2$^{-/-}$ mice and incubated with AcLDL (25 μg/ml) for 48 h. *A* and *B*, following two washes with PBS, cells were either fixed and stained with Oil Red O (*A*) or used for total lipid extraction and cholesterol mass measurement (*B*). Total cholesterol mass was normalized to total cellular protein, and data (mean ± S.D., $n = 6$) are presented as nanomoles per milligram of protein. *C*, total protein extracts of macrophages were subjected to Western blot analyses to assess SR-A expression; β-actin was used as a loading control. *D*, for measurement of cholesterol efflux, cells were loaded with AcLDL and labeled with [^{3}H]-cholesterol for 48 h. Following a 24-h equilibration, cholesterol efflux to 10% FBS in the growth medium was monitored over time. Data (mean ± S.D., $n = 6$) are presented as percent efflux. *, $p < 0.05$.

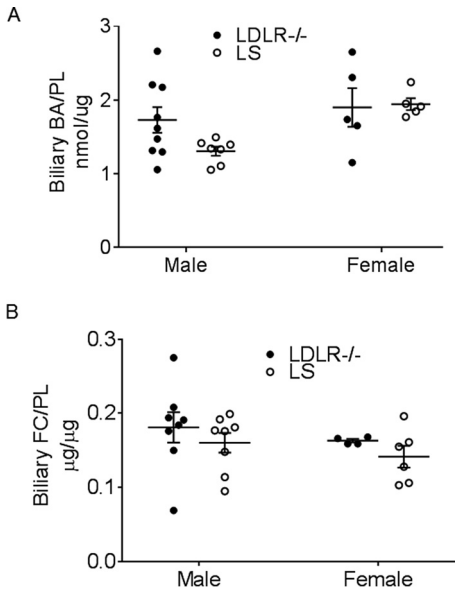

Figure 8. Effects of SCP2 deficiency on biliary bile acid and cholesterol secretion. *A* and *B*, gall bladder bile was collected at the time of euthanasia, and the total volume was noted. Biliary bile acids (*BA*), cholesterol, and phospholipids (*PL*) were estimated as described under "Experimental procedures." Data are presented as total bile acids (nanomoles) or FC (micrograms) in the bile normalized to total phospholipids (micrograms) in *A* and *B*, respectively.

expression of SCP-2 in rat small intestine enterocytes and, based on the intracellular distribution, suggested that this protein may play a role in the intracellular processing of absorbed lipids. The data presented here show that SCP2/SCPx deficiency significantly reduces intestinal cholesterol absorption and that siRNA-dependent knockdown of SCP2 in human intestinal epithelial cells leads to a significant reduction in cholesterol accumulation, indicating that intestinal SCP2 regulates the uptake of dietary cholesterol and is likely responsible for the reduced plasma lipids in LS mice. Future development of an intestine-specific SCP2 knockout will facilitate the direct confirmation of this hypothesis. Reduction in cholesterol absorption is used as a clinical intervention, and supplementation with ezetimibe reduced plasma cholesterol by 32%, leading to a reduction in atherosclerosis by 52–59% in LDLR$^{-/-}$ mice (22). The data presented here are not only consistent with these observations but also show a more pronounced effect of SCP2

deficiency on plasma cholesterol (a >70% decrease in LS mice) and atherosclerosis (a >80% reduction in total lesion area), underscoring the need to evaluate intestinal SCP2 inhibition as a potential anti-atherosclerotic strategy.

The liver plays a major role in regulating whole-body lipid homeostasis by secreting triglyceride-rich and atherogenic lipoproteins (VLDL) and eliminating cholesterol returning to the liver via LDL or HDL in bile. Earlier studies by Martin *et al.* (17) have demonstrated no change in the expression of ApoB100/ApoB48 protein or MTP mRNA levels in SCP2/SCPx-deficient mice. Accordingly, it was concluded that aberration in the intracellular transfer of fatty acids and cholesterol because of SCP2/SCPx deficiency likely affects synthesis of triglycerides or cholesteryl esters required for normal secretion of lipidated ApoB100 or VLDL particles. Consistently, in this study, we demonstrate a significant reduction in triglyceride/VLDL secretion in SCP2$^{-/-}$ mice. Furthermore, a significant reduction was also observed in [^{3}H]oleic acid incorporation in triglycerides as well as cholesteryl esters by SCP2$^{-/-}$ hepatocytes and decreased uptake of [^{3}H]cholesterol *in vivo* or by SCP2 knockdown in intestinal epithelial cells. Taken together with the established role of SCP-2 in intracellular transport of cholesterol and fatty acids, these data provide additional support for the proposed concept that SCP2 is required for triglyceride and cholesteryl ester synthesis (both in liver as well as intestinal cells) and that its deficiency leads to impaired chylomicron or VLDL secretion.

Despite the predicted role of SCP2 in delivering cholesterol to the endoplasmic reticulum for bile acid synthesis and of SCPx thiolase in bile acid synthesis (23), deficiency of SCP2/SCPx in LS mice did not affect biliary bile acid secretion, indicating a limited role, if any, of increased biliary elimination of cholesterol as a possible mechanism for the observed reduction in atherosclerosis. Fuchs *et al.* (24) have also reported lower bile salt secretion rates in SCP2$^{-/-}$ mice, resulting in a lower bile salt pool size. Furthermore, SCP2/SCPx deficiency did not affect the secretion of cholesterol into the bile, consistent with the reported lack of changes in Abcg5 and Abcg8 expression in these mice (17). It is noteworthy that SCP2/SCPx deficiency leads to an increase in liver fatty acid binding protein or FABP-1, speculated to compensate for some of the functions of hepatic SCP2 (23).

Although it is beyond the scope of this study to examine the various other physiological functions attributed to SCP2, it is noteworthy that cells overexpressing SCP2 become more susceptible to damage/toxicity by 7α-OOH, a free radical generated by cholesterol hydroperoxides, because cellular SCP2 binds and traffics 7α-OOH to mitochondria, where it exerts cellular toxicity (25). Whether reduction in SCP2-mediated cytotoxicity underlies the observed reduction in plaque necrosis remains to be established. Based on the subcellular localization of SCPx in peroxisomes and its demonstrated role in modulating peroxisomal fatty acid oxidation, Seedorf *et al.* (26) hypothesized that SCP2 functions *in vivo* as fatty acyl–CoA carrier. Future studies designed to specifically examine peroxisomal function will determine whether SCPx deficiency–mediated perturbations of peroxisomal fatty acid metabolism contribute to the observed reduction in atherosclerosis.

In conclusion, the data presented here provide very strong evidence for the pro-atherogenic role of SCP2 by demonstrating a dramatic reduction in diet-induced atherosclerosis in SCP2/SCPx– deficient mice in the LDLR$^{-/-}$ background. Furthermore, the dramatic lipid-lowering effects of SCP2 deficiency despite WD feeding provide a novel opportunity to develop SCP2 inhibitors for attenuation of WD-induced dyslipidemia and downstream adverse effects such as development of atherosclerosis.

Experimental procedures

Animals

LDLR$^{-/-}$ mice were obtained from The Jackson Laboratory. We obtained the first generation of SCP2/SCPx$^{-/-}$ mice (designated SCP2$^{-/-}$) from the Mutant Mouse Resource and Research Center (MMRRC) (Chapel Hill, NC) after these strains were deposited at this consortium by Dr. Schroeder's laboratory. All mice were maintained in a helicobacter-free barrier facility at VCU. All experimental procedures were approved by the VCU Institutional Animal Care and Use Committee.

Development of experimental animals

SCP2$^{-/-}$ mice were crossed into the LDLR$^{-/-}$ background, and the resulting LDLR$^{-/-}$SCP2$^{-/-}$ mice were designated LS. Male and female mice were included in the study at 10 weeks of age, and the total number of animals in each group was, therefore, determined by the availability of each gender within a litter. For assessment of atherosclerosis, mice were fed a Western-type high-fat/high-cholesterol diet (TD88137, Harlan Teklad) that contains 21% fat, 0.15% cholesterol, and 19.5% casein by weight with no sodium cholate for 16 weeks.

Quantitative atherosclerosis analyses

The aorta was dissected from the heart to the iliac bifurcation, cleaned of any surrounding tissue, opened longitudinally, pinned on black wax, and fixed for 24 h in 10% buffered formalin. The fixed aortae were imaged on a black background using a Canon digital camera fitted with a 60-mm f/2.8 macro lens. The total area and the area occupied by the lesions in the aortic arch and total aorta were determined using AxioVision^{TM} image analysis software. The person quantifying the area occupied by lesions was blinded to the identity of the images.

Morphological analyses of the lesions

Hearts were fixed in buffered formalin, paraffin-embedded, and sectioned. When the aortic sinus was visible, three to four serial sections (5 μm thick) were transferred to numbered slides. The slides were then either stained with hematoxylin and eosin (H&E) or Masson's trichrome stain, and images were acquired using a Zeiss inverted microscope fitted with a digital camera as described earlier (27).

Cholesterol loading and efflux assays

Thioglycolate-elicited mouse peritoneal macrophages were obtained from either C57BL/6 (WT) or SCP2$^{-/-}$ mice and incubated with AcLDL (25 μg/ml) for 48 h. Following two

washes in PBS, cells were either fixed in 10% buffered formalin to stain with Oil Red O (28) or used for total lipid extraction and estimation of cholesterol mass free using reverse phase-HPLC. Total cellular protein was estimated following lipid extraction using a Bio-Rad dye binding assay. Cholesterol efflux was monitored as described before (29).

Hepatic VLDL secretion in vivo

C57BL/6 (WT) or SCP2$^{-/-}$ mice were fasted overnight, and a baseline blood sample was collected from the tail vein. Mice were subsequently injected intravenously with the lipoprotein lipase inhibitor tyloxapol (500 mg/kg) in PBS, and blood samples were collected over a period of 3 h. Plasma triglyceride levels, a measure of plasma VLDL, were measured using the L-Type Triglyceride M kit from Wako Diagnostics. The VLDL secretion rate was calculated as described previously (30).

Lipid secretion from hepatocytes

Primary mouse hepatocytes were prepared as described earlier (31). After 24 h, the medium was replaced with fresh William's E growth medium containing 200 μM oleic acid–BSA (Sigma) and [^{3}H]oleic acid (5 μCi/ml). After 4 h, the medium was replaced with fresh growth medium without [^{3}H]oleic acid (5 μCi/ml), and incubation continued for an additional 4 h. Total lipid were extracted from the conditioned medium, and neutral lipid was separated by TLC using hexane:diethylether: acetic acid 90:10:1 (v/v) as the solvent system (32). Percent [^{3}H]incorporation into triglycerides and cholesteryl esters was normalized to total cellular protein.

Cholesterol absorption

C57BL/6 (WT) or SCP2$^{-/-}$ mice were fasted overnight and then injected intravenously with tyloxapol (500 mg/kg) in PBS to inhibit lipoprotein lipase. After 10 min, mice were gavaged with 200 μl of olive oil containing 2 μCi [^{3}H]cholesterol. Mice were euthanized after 5 h, and blood was collected. Radioactivity associated with plasma was determined by liquid scintillation counting, and data are presented as plasma DPM per microliter of plasma.

SCP2 knockdown and uptake of cholesterol by intestinal epithelial cells

The human intestinal epithelial cell line (HT29) was obtained from the ATCC and maintained in McCoy's 5A medium containing 10% FBS and penicillin/streptomycin (100 units/ml and 100 μg/ml). Cells were plated at a density of 0.5×10^5 cells/well into 24-well plates and 0.5×10^6 cells/well into 6-well plates and cultured for ~20 h to reach ~60% confluence. Cells were transfected with a complex consisting of SCP2 siRNA (Santa Cruz Biotechnology, catalog no. sc-44636) and polyamidoamine (PAMAM) G5 (Sigma-Aldrich). Each component was diluted in 200 μl McCoy's 5A medium and mixed by vortexing for 1 min at the appropriate weight ratio of siRNA to polyamidoamine G5 as 1:10. Following incubation at room temperature for 30 min, the resulting complexes were added to cells. The medium was replaced with normal growth medium, and cells were harvested after an additional 24 h to monitor knockdown of SCP2 expression. Quantitative RT-PCR was used to measure mRNA levels using a TaqMan assay (Hs00920780_m1), and the protein levels were measured by Western blot analyses using primary antibody 23006-1-AP (Proteintech Group), which recognizes both SCP2 and SCPx. For measurement of cholesterol uptake, 24 h after transfection, the medium was replaced with growth medium containing 1% FBS and [^{3}H]cholesterol (1 μCi/ml). Cells were harvested at 15, 30, and 60 min and lysed in radioimmune precipitation assay buffer, and associated radioactivity was determined by liquid scintillation counting and normalized to total cellular protein.

Gene expression analyses

Total RNA from the liver or different segments of the gastrointestinal tract was prepared using RNeasy mini kits (Qiagen), and the mRNA levels of the indicated genes were determined using optimized TaqMan probe sets from Applied Biosystems: Abcg5, Mm00446249_m1; Abcg8, Mm00445970_m1; ApoB, Mm01545156_m1; Fas, Mm00662319_m1; Npc1l1, Mm01191973_m1; Scp-2, Mm01257982_m1; Srebp-1c, Mm00550338_m1; and Srebp-2, Mm01306292_m1.

Analytical methods

Total bile acid levels in gall bladder bile were determined using the bile acid quantification kit from Trinity Biotech (Wicklow, Ireland). Phospholipid content was measured using the Phospholipid C kit from Wako Diagnostics (Richmond, VA). Total cholesterol (in plasma and bile) and total triglyceride levels (in plasma) were determined using the Cobas c311 automated chemistry analyzer, with reagents, calibrators, and controls from Roche Diagnostics. To correct for likely differences because of the concentration of bile in the gall bladder, bile acid and cholesterol content in total bile was normalized to total phospholipid (nanomoles per microgram). HDL and non-HDL (VLDL and LDL)–associated cholesterol was determined using a kit from Abcam.

Statistics

All data were analyzed using GraphPad Prism software. Statistical significance of differences between two groups was determined by two-way analysis of variance, and Tukey's multiple comparisons tests were performed to evaluate the significant difference between groups. Significance of differences between two groups was determined using nonparametric t test, and $p < 0.05$ was considered statistically significant.

Author contributions—H. H., J. W., and S. G. investigation; H. H., J. W., G. K., W. J. K., and S. G. methodology; P. J. Y. and S. G. formal analysis; S. G. conceptualization; S. G. supervision; S. G. funding acquisition; S. G. writing-original draft; S. G. project administration; S. G. writing-review and editing.

Acknowledgments—We thank Dr. Freidhelm Schroeder for providing timely information on the deposition of SCP2$^{-/-}$ mice to the MMRRC, making it possible to obtain these mice.

References

1. Phillips, M. C., Johnson, W. J., and Rothblat, G. H. (1987) Mechanisms and consequences of cellular cholesterol exchange and transfer. *Biochim. Biophys. Acta* **906,** 223–276 CrossRef Medline

2. Zilversmit, D. B. (1984) Lipid transfer proteins. *J. Lipid Res.* **25,** 1563–1569 Medline
3. Soccio, R. E., and Breslow, J. L. (2003) StAR-related lipid transfer (START) proteins: mediators of intracellular lipid metabolism. *J. Biol. Chem.* **278,** 22183–22186 CrossRef Medline
4. Scallen, T. J., Pastuszyn, A., Noland, B. J., Chanderbhan, R., Kharroubi, A., and Vahouny, G. V. (1985) Sterol carrier and lipid transfer proteins. *Chem. Phys. Lipids* **38,** 239–261 CrossRef Medline
5. Gallegos, A. M., Atshaves, B. P., Storey, S. M., Starodub, O., Petrescu, A. D., Huang, H., McIntosh, A. L., Martin, G. G., Chao, H., Kier, A. B., and Schroeder, F. (2001) Gene structure, intracellular localization, and functional roles of sterol carrier protein-2. *Prog. Lipid Res.* **40,** 498–563 CrossRef Medline
6. Chanderbhan, R. F., Kharroubi, A. T., Noland, B. J., Scallen, T. J., and Vahouny, G. V. (1986) Sterol carrier protein 2: further evidence for its role in adrenal steroidogenesis. *Endocr. Res.* **12,** 351–370 CrossRef Medline
7. Ohba, T., Rennert, H., Pfeifer, S. M., He, Z., Yamamoto, R., Holt, J. A., Billheimer, J. T., and Strauss, J. F., 3rd. (1994) The structure of the human sterol carrier protein X/sterol carrier protein 2 gene (SCP2). *Genomics* **24,** 370–374 CrossRef Medline
8. Schroeder, F., Frolov, A. A., Murphy, E. J., Atshaves, B. P., Jefferson, J. R., Pu, L., Wood, W. G., Foxworth, W. B., and Kier, A. B. (1996) Recent advances in membrane cholesterol domain dynamics and intracellular cholesterol trafficking. *Proc. Soc. Exp. Biol. Med.* **213,** 150–177 CrossRef Medline
9. Gallegos, A. M., Schoer, J. K., Starodub, O., Kier, A. B., Billheimer, J. T., and Schroeder, F. (2000) A potential role for sterol carrier protein-2 in cholesterol transfer to mitochondria. *Chem. Phys. Lipids* **105,** 9–29 CrossRef Medline
10. Schroeder, F., Atshaves, B. P., McIntosh, A. L., Gallegos, A. M., Storey, S. M., Parr, R. D., Jefferson, J. R., Ball, J. M., and Kier, A. B. (2007) Sterol carrier protein-2: new roles in regulating lipid rafts and signaling. *Biochim. Biophys. Acta* **1771,** 700–718 CrossRef Medline
11. Roff, C. F., Pastuszyn, A., Strauss, J.F., 3rd, Billheimer, J. T., Vanier, M. T., Brady, R. O., Scallen, T. J., and Pentchev, P. G. (1992) Deficiencies in sex-regulated expression and levels of two hepatic sterol carrier proteins in a murine model of Niemann-Pick type C disease. *J. Biol. Chem.* **267,** 15902–15908
12. Atshaves, B. P., McIntosh, A. L., Martin, G. G., Landrock, D., Payne, H. R., Bhuvanendran, S., Landrock, K. K., Lyuksyutova, O. I., Johnson, J. D., Macfarlane, R. D., Kier, A. B., and Schroeder, F. (2009) Overexpression of sterol carrier protein-2 differentially alters hepatic cholesterol accumulation in cholesterol-fed mice. *J. Lipid Res.* **50,** 1429–1447 CrossRef Medline
13. Storey, S. M., McIntosh, A. L., Huang, H., Landrock, K. K., Martin, G. G., Landrock, D., Payne, H. R., Atshaves, B. P., Kier, A. B., and Schroeder, F. (2012) Intracellular cholesterol-binding proteins enhance HDL-mediated cholesterol uptake in cultured primary mouse hepatocytes. *Am. J. Physiol. Gastrointest. Liver Physiol.* **302,** G824–G839
14. Wang, J., Bie, J., and Ghosh, S. (2016) Intracellular cholesterol transport proteins enhance hydrolysis of HDL-CEs and facilitate elimination of cholesterol into bile. *J. Lipid Res.* **57,** 1712–1719 CrossRef Medline
15. Martin, G. G., Atshaves, B. P., Landrock, K. K., Landrock, D., Storey, S. M., Howles, P. N., Kier, A. B., and Schroeder, F. (2014) Ablating L-FABP in SCP-2/SCP-x null mice impairs bile acid metabolism and biliary HDL-cholesterol secretion. *Am. J. Physiol. Gastrointest. Liver Physiol.* **307,** G1130–G1143 CrossRef Medline
16. Martin, G. G., Landrock, D., Landrock, K. K., Howles, P. N., Atshaves, B. P., Kier, A. B., and Schroeder, F. (2015) Relative contributions of L-FABP, SCP-2/SCP-x, or both to hepatic biliary phenotype of female mice. *Arch. Biochem. Biophys.* **588,** 25–32 Medline
17. Martin, G. G., Atshaves, B. P., Landrock, K. K., Landrock, D., Schroeder, F., and Kier, A. B. (2015) Loss of L-FABP, SCP-2/SCP-x, or both induces hepatic lipid accumulation in female mice. *Arch. Biochem. Biophys.* **580,** 41–49 CrossRef Medline
18. Huszar, D., Varban, M. L., Rinninger, F., Feeley, R., Arai, T., Fairchild-Huntress, V., Donovan, M. J., and Tall, A. R. (2000) Increased LDL cholesterol and atherosclerosis in LDL receptor-deficient mice with attenuated expression of scavenger receptor B1. *Arterioscler. Thromb. Vasc. Biol.* **20,** 1068–1073 CrossRef Medline
19. Billheimer, J. T., and Reinhart, M. P. (1990) Intracellular trafficking of sterols. *Subcell. Biochem.* **16,** 301–331 CrossRef Medline
20. Kharroubi, A., Wadsworth, J. A., Chanderbhan, R., Wiesenfeld, P., Noland, B., Scallen, T., Vahouny, G. V., and Gallo, L. L. (1988) Sterol carrier protein2-like activity in rat intestine. *J. Lipid Res.* **29,** 287–292 Medline
21. Wouters, F. S., Markman, M., de Graaf, P., Hauser, H., Tabak, H. F., Wirtz, K. W., and Moorman, A. F. (1995) The immunohistochemical localization of the non-specific lipid transfer protein (sterol carrier protein-2) in rat small intestine enterocytes. *Biochim. Biophys. Acta* **1259,** 192–196 CrossRef Medline
22. Basso, F., Freeman, L. A., Ko, C., Joyce, C., Amar, M. J., Shamburek, R. D., Tansey, T., Thomas, F., Wu, J., Paigen, B., Remaley, A. T., Santamarina-Fojo, S., and Brewer, H. B., Jr. (2007) Hepatic ABCG5/G8 overexpression reduces apoB-lipoproteins and atherosclerosis when cholesterol absorption is inhibited. *J. Lipid Res.* **48,** 114–126 Medline
23. Kannenberg, F., Ellinghaus, P., Assmann, G., and Seedorf, U. (1999) Aberrant oxidation of the cholesterol side chain in bile acid synthesis of sterol carrier protein-2/sterol carrier protein-x knockout mice. *J. Biol. Chem.* **274,** 35455–35460 CrossRef Medline
24. Fuchs, M., Hafer, A., Münch, C., Kannenberg, F., Teichmann, S., Scheibner, J., Stange, E. F., and Seedorf, U. (2001) Disruption of the sterol carrier protein 2 gene in mice impairs biliary lipid and hepatic cholesterol metabolism. *J. Biol. Chem.* **276,** 48058–48065 CrossRef Medline
25. Kriska, T., Levchenko, V. V., Korytowski, W., Atshaves, B. P., Schroeder, F., and Girotti, A. W. (2006) Intracellular dissemination of peroxidative stress: internalization, transport, and lethal targeting of a cholesterol hydroperoxide species by sterol carrier protein-2-overexpressing hepatoma cells. *J. Biol. Chem.* **281,** 23643–23651 CrossRef Medline
26. Seedorf, U., Ellinghaus, P., and Roch Nofer, J. (2000) Sterol carrier protein-2. *Biochim. Biophys. Acta* **1486,** 45–54 CrossRef Medline
27. Zhao, B., Song, J., Chow, W. N., St Clair, R. W., Rudel, L. L., and Ghosh, S. (2007) Macrophage-specific transgenic expression of cholesteryl ester hydrolase significantly reduces atherosclerosis and lesion necrosis in Ldlr mice. *J. Clin. Invest.* **117,** 2983–2992 CrossRef Medline
28. Ghosh, S., St Clair, R. W., and Rudel, L. L. (2003) Mobilization of cytoplasmic CE droplets by overexpression of human macrophage cholesteryl ester hydrolase. *J. Lipid Res.* **44,** 1833–1840 CrossRef Medline
29. Zhao, B., Song, J., St Clair, R. W., and Ghosh, S. (2007) Stable overexpression of human macrophage cholesteryl ester hydrolase results in enhanced free cholesterol efflux from human THP1 macrophages. *Am. J. Physiol. Cell Physiol.* **292,** C405–C412 CrossRef Medline
30. Coenen, K. R., Gruen, M. L., and Hasty, A. H. (2007) Obesity causes very low density lipoprotein clearance defects in low-density lipoprotein receptor-deficient mice. *J. Nutr. Biochem.* **18,** 727–735 CrossRef Medline
31. Hylemon, P. B., Gurley, E. C., Kubaska, W. M., Whitehead, T. R., Guzelian, P. S., and Vlahcevic, Z. R. (1985) Suitability of primary monolayer cultures of adult rat hepatocytes for studies of cholesterol and bile acid metabolism. *J. Biol. Chem.* **260,** 1015–1019 Medline
32. Bie, J., Zhao, B., Marqueen, K. E., Wang, J., Szomju, B., and Ghosh, S. (2012) Macrophage-specific transgenic expression of cholesteryl ester hydrolase attenuates hepatic lipid accumulation and also improves glucose tolerance in ob/ob mice. *Am. J. Physiol. Endocrinol. Metab.* **302,** E1283–E1291 CrossRef Medline